Development 130, 2695-2704

doi:10.1242/dev.00509

The *Xenopus* LIM-homeodomain protein Xlim5 regulates the differential adhesion properties of early ectoderm cells

Douglas W. Houston and Christopher Wylie*

Division of Developmental Biology MLC 7007, Cincinnati Children's Hospital Medical Center, 3333 Burnet Avenue, Cincinnati, OH 45229-3039, USA

*Author for correspondence (e-mail: Christopher.Wylie@chmcc.org)

Accepted 26 March 2003

SUMMARY

One of the earliest lineage restriction events in embryogenesis is the specification of the primary germ layers: ectoderm, mesoderm and endoderm. In *Xenopus*, germ layer specification occurs prior to gastrulation and requires the transcription factor VegT both for the cell-autonomous specification of endoderm and the generation of mesoderm-inducing signals. In the absence of VegT, ectoderm is formed in all regions of the embryo. In this work, we show that VegT-depleted vegetal cells (prospective endoderm) behave like animal cells in sorting assays and ectopically express early markers of ectoderm. To gain insight into how ectoderm is specified, we looked for candidate ectoderm-specific genes that are ectopically expressed in VegT-depleted embryos, and examined the role of one of these, the LIM homeobox gene *Xlim5*, in ectoderm development. We show that overexpression of *Xlim5* in prospective endoderm cells is sufficient to impair sorting of animal cells from vegetal cells but is not sufficient (at similar doses) to induce ectoderm-specific genes. In whole embryos, *Xlim5* causes vegetal cells to segregate inappropriately to other germ layers and express late differentiation markers of that germ layer. Inhibition of Xlim5 function using an Engrailed repressor construct or a morpholino oligonucleotide causes loss of animal cell adhesion or delay in neural fold morphogenesis, respectively, without significantly affecting early ectoderm gene expression. Taken together, our results provide evidence that a primary role for Xlim5 is to specifically regulate differential cell adhesion behaviour of the ectoderm.

Key words: Adhesion, Ectoderm, Germ layer, LIM homeobox, VegT, *Xenopus*

INTRODUCTION

One of the principal events in early vertebrate development is the organization of the three primary germ layers during gastrulation. Each adult tissue is derived from one of the three germ layers, so an understanding of germ layer specification is crucial to the understanding of subsequent tissue formation. In *Xenopus*, cells of the late blastula are regionally specified according to their germ layer fate in the embryo. Animal cells form ectoderm (nervous tissue and epidermis), equatorial cells form mesoderm (notochord, muscle, mesenchyme and blood) and the vegetal cells form endoderm (the lining of the gut and organs derived from it) (Heasman, 1997). Several experiments indicate that germ layer identity is established by the late blastula stage. First, explants of the animal, equatorial and vegetal regions develop in isolation as ectoderm, mesoderm and endoderm, respectively. Second, transplantation experiments showed that single blastomeres, irrespective of origin, could contribute to all three germ layers during the early blastula stage (Heasman et al., 1984; Snape et al., 1987). By late blastula, however, transplanted cells segregate to individual germ layers depending on their origin (Heasman et al., 1984; Snape et al., 1987; Wylie et al., 1987). In addition, disaggregated late blastula cells from different regions of the embryo sort out from each other in culture (Turner et al., 1989). Thus, the primary germ layers are identifiable by their differential adhesion properties by late blastula, prior to any overt differentiation or morphogenesis.

In *Xenopus*, the primary germ layers are thought to be determined by the cytoplasmic localization of maternal determinants and subsequent cell-cell communication. Of the three germ layers, only the formation of mesoderm and endoderm are understood, whereas very little is known about specification of the ectoderm. Equatorial cells in the blastula form mesoderm in response to signalling by zygotic TGF-β-related growth factors released by the vegetal cells. The T-box transcription factor VegT, which is encoded by a vegetally localized RNA, is required for the specification of endoderm in the vegetal hemisphere and is necessary for the generation of mesoderm- and endoderm-inducing signals (Xanthos et al., 2001; Kofron et al., 1999; Zhang et al., 1998). In addition, both mesoderm and endoderm require cell-cell communication prior to gastrulation for the formation of differentiated cell types (Lemaire and Gurdon, 1994; Yasuo and Lemaire, 1999).

In the absence of *VegT*, vegetal and marginal cells express ectodermal genes (Zhang et al., 1998). Once specified as

ectoderm, cells differentiate either as epidermis if BMP signalling is active or as neural tissue if BMP signalling is absent; termed the 'default state' model (reviewed by Muñoz-Sanjuan and Brivanlou, 2002). In contrast to mesoderm and endoderm, and consistent with the default model, ectoderm can form in the absence of cell-cell contact (Wilson and Hemmati-Brivanlou, 1995), suggesting that maternal, cell autonomous factors are responsible for ectoderm specification. Such factors must be present throughout the embryo because ectoderm can be ectopically induced in vegetal explants (which normally form endoderm) by depletion of maternal *VegT* RNA (Zhang et al., 1998) or by overexpression of TGFβ signalling antagonists (Henry et al., 1996).

In this work we focus on identifying factors involved in the genetic program of ectoderm specification. We looked for transcription factors upregulated in *VegT*-depleted vegetal explants as potential factors downstream of the ectoderm specification pathway. We identified *Xlim5*, a LIM-homeobox encoding gene as one such factor. *Xlim5* was originally identified by its close sequence similarity to *Xlim1* (Toyama et al., 1995) and is expressed throughout the gastrula ectoderm before becoming restricted to the anterior neural plate and later to the brain and spinal cord. LIM-homeodomain proteins (LIM HD or Lhx proteins) have been identified as important developmental regulators in many cell types and contain two zinc-finger LIM domains followed by a homeodomain (reviewed by Hobert and Westphal, 2000). We show that overexpression of *Xlim5* in vegetal cells (prospective endoderm) interferes with the ability of vegetal cells to segregate from animal cells in cell-sorting assays without inducing ectoderm markers. *Xlim5* expression in whole embryos causes vegetal cells to relocate to ectoderm- and mesoderm-derived regions and express late differentiation markers of these tissues. Interference with Xlim5 function, using an Engrailed repressor construct, or blockage of its translation with antisense morpholino (MO) oligonucleotides, results in defects in ectoderm cell adhesion or neural plate morphogenesis, respectively, without affecting the initial formation of the ectoderm germ layer. These data provide evidence that *Xlim5* regulates differential adhesion properties of animal cells in the blastula but may not be required for other aspects of ectoderm fate specification.

MATERIALS AND METHODS

Oocytes and embryos

Manually defolliculated oocytes were injected vegetally with VegT oligos (7 ng) or *Xlim5-EnR* RNA (1 ng), cultured at 18°C in oocyte culture medium (OCM) and fertilized using the host transfer technique as described (Zuck et al., 1998). Eggs were stripped and fertilized using a sperm suspension and embryos were maintained in 0.2×MMR. For mRNA or morpholino oligonucleotide (MO) injections after fertilization, embryos were dejellied and transferred to 2% Ficoll in 0.5×MMR prior to injection. For explant assays, vegetal masses were dissected from stage 9 embryos on agarose-coated dishes in 1×MMR and cultured to the desired stage in OCM.

Blastomere-sorting assays were performed essentially as described (Turner et al., 1989). In the *VegT* experiments, control uninjected or *VegT*-depleted embryos were injected vegetally with 1 ng of rhodamine-conjugated dextran (RLDX; Molecular Probes). At the early gastrula stage, embryos were dissociated on agarose-coated dishes in 67 mM phosphate buffer (pH 7.4) and transferred to Ca^{2+}-Mg^{2+}-free medium [CMFM; 7.5 mM Tris (pH 7.6), 88 mM NaCl, 1 mM KCl, 2.4 mM $NaHCO_3$]. Various combinations of blastomeres were mixed and reaggregated in OCM in small wells in agarose dishes. Aggregates were incubated 4 hours to overnight before they were fixed in MEMFA, dehydrated in methanol, cleared in Murray's clear (1:2 benzyl alcohol:benzyl benzoate) and visualized by confocal microscopy (Zeiss LSM 510). The *Xlim5* experiments were carried similarly except that RNAs were injected vegetally and RLDX was injected animally. For timelapse movies, cells were labelled in 10 μg/ml tetramethyl rhodamine isothiocyanate (TRITC) as described (Turner et al., 1989) and filmed using the Axiovision software (Zeiss) on an Axiovert 100M microscope with a rhodamine filter set. Frames were collected every 20 seconds over a 1 hour period and assembled into movies using Quicktime software (Apple Computer). Dissociated cells were stained with Sytox Green at a concentration of 1 μM, according to the manufacturer's instructions (Molecular Probes).

Oligos and mRNAs

The antisense oligodeoxynucleotides used were HPLC-purified phosphorothioate-phosphodiester chimeric oligonucleotides (Sigma/Genosys) with the base composition:VegT (VT9M): 5′-C*A*G*CA-GCATGTACTT*G*G*C-3′ (Zhang et al., 1998). Asterisks represent phosphorothioate bonds. Oligos were resuspended in sterile, filtered water. An antisense MO against *Xlim5* was obtained from Gene-Tools: Xlim5-MO: 5′-TCATAGACTCCCCAACCAAAGACCC-3′.

This MO binds at nucleotide 491 of the full-length *Xlim5* sequence (start codon is nucleotide 561).

Full-length *Xlim5* was obtained by PCR from stage 10 cDNA, cloned into pCRII-TOPO according to the manufacturer's instructions (Invitrogen) and sequenced. A region containing the *Xlim5*-coding region was cloned into pCS2+ by digesting with internal *Pvu*II and *Hin*cII sites and ligating to *Stu*I digested pCS2+. This cDNA begins at nucleotide 545 and does not contain the MO-binding sequence. The Engrailed repressor domain was fused to Xlim5 C-terminal to the homeodomain by subcloning a *Bam*HI-*Afe*I fragment of pCS2+Xlim5 into *Bgl*II-*Sma*I digested pEnR/RN3P1.1 (Ryan et al., 1996). *Xlim5* mRNA was synthesized from *Not*I-linearized template using the SP6 mMessage mMachine kit (Ambion). *Xlim5-EnR* and control *EnR* RNA (pEnβ1) were *Sfi*I digested and transcribed with a T3 kit. RNAs were LiCl precipitated and resuspended in sterile distilled water.

Analysis of gene expression using real-time RT-PCR

Total RNA was prepared from oocytes, embryos and explants using proteinase K, and then treated with RNase-free DNase as described (Zhang et al., 1998). Approximately one-sixth embryo equivalent of RNA was used for cDNA synthesis with oligo(dT) primers followed by real-time RT-PCR and quantitation using the LightCycler™ System (Roche) as described previously (Kofron et al., 2001). The primers and cycling conditions used are listed in Table 1. Relative expression values were calculated by comparison with a standard curve generated by serial dilution of uninjected control cDNA. Samples were normalized to levels of *ornithine decarboxylase* (*ODC*). Samples of water alone or controls lacking reverse transcriptase in the cDNA synthesis reaction failed to give specific products in all cases. The cDNA used in Fig. 2B was generated previously (Kofron et al., 1999) and was reassayed for *Xlim5* expression.

Lineage analysis

Injection of *β-galactosidase* (*β-gal*) RNA was used to follow the fate of otherwise uninjected or *Xlim5*-co-injected cells. The presence of *β-gal* in embryos was detected by whole-mount X-gal staining. These embryos were refixed, dehydrated, cleared in Histoclear, embedded in paraffin wax and sectioned. For analysis of germ layer-specific markers in *β-gal*-injected cells, embryos were subjected to cryosectioning and immunostaining. Embryos were fixed for 2 hours at 4°C in 2% TCA (in water) and equilibrated in 15% sucrose for 1

hour followed by 30% sucrose overnight. The embryos were then embedded in 7.5% gelatin in 15% sucrose prior to equilibration in OCT freezing medium and cryosectioning. Sections were stained for 4 hours to overnight with primary antibodies diluted in PGT (1×PBS, pH 7.4, 1% goat serum, 0.1% Triton X-100), washed three times for 5 minutes in PBS and stained for 2 hours in secondary antibodies. Slides were washed as above, mounted in 50% glycerol containing 100 μg/ml DABCO (Sigma) and examined by confocal microscopy. Antibodies used were mAb 12/101 (1:10), rabbit-anti-β-galactosidase (1:500; Molecular Probes), Cy2-conjugated goat anti-rabbit and Cy5-conjugated goat anti-mouse (1:50 and 1:100, respectively; Jackson Immunoresearch).

RESULTS

Depletion of *VegT* confers ectoderm cell adhesion properties on vegetal blastomeres

Embryos depleted of maternal *VegT* RNA ectopically express ectodermal genes, both neural and epidermis specific, in vegetal cells normally fated to form endoderm (Zhang et al., 1998). Because other localized determinants are present in vegetal cells, we wished to know to what extent ectopic ectoderm gene expression correlated with ectodermal cell behaviour in *VegT*-depleted embryos. We first performed blastomere-sorting assays to determine if *VegT*-depleted vegetal cells acquire the adhesion properties of ectoderm cells in addition to expressing ectodermal genes. Dissaggregated vegetal cells from either *VegT*-depleted or control gastrulae labelled with RLDX were mixed with unlabelled dissaggregated animal or vegetal cells, and allowed to reaggregate for 4 hours to overnight. Aggregates were then fixed and cleared and sorting was scored by confocal microscopy. The numbers given below are from two independent experiments. Control animal cells sorted well from vegetal cells (10/10 cases; Fig. 1A), but not from other vegetal cells (10/10 cases; Fig. 1B). Animal cells were unable to sort from *VegT*-depleted vegetal cells as evidenced by a random mixing of labelled and unlabelled cells (Fig. 1C,C′; positive sorting in 2/10 cases). Surprisingly, *VegT*-depleted vegetal cells did not sort from control vegetal cells (Fig. 1D,D′; 0/8 positive sorting for both controls and *VegT* depleted).

VegT-depleted vegetal cells express the LIM-homeobox gene *Xlim5*

To identify candidate genes controlling differential adhesion behaviour in the early ectoderm, we assayed *VegT*-depleted vegetal explants during the gastrula stages for the expression of potential ectoderm regulatory genes by real-time RT-PCR. Through a search of the literature, we identified *Xlim5* as such a candidate based on its published expression pattern (Toyama et al., 1995). We found that expression of *Xlim5*, which encodes a LIM-homeodomain protein (Toyama et al., 1995), was increased in both *VegT*-depleted whole embryos and in isolated vegetal masses from *VegT*-depleted embryos (Fig. 2A). During normal development, *Xlim5* is expressed throughout the gastrula ectoderm and gradually becomes restricted to neurones late in neurulation (Toyama et al., 1995). We assayed additional ectodermal markers, *Epidermal keratin* and *E-cadherin*, and found them to be similarly affected (Fig. 2A).

Ectopic expression of *Xlim5* in *VegT*-depleted vegetal explants could arise because either VegT or its downstream targets, such as *Xenopus nodal*-related genes (*Xnrs*), are normally required to repress ectoderm gene expression vegetally. Consistent with this idea, Toyama et al. (Toyama et al., 1995) showed that *Xlim5* expression was inhibited by activin. To test whether *nodal*-related genes could also inhibit *Xlim5* expression, we examined *Xlim5* expression in *VegT*-depleted embryos and *VegT*-depleted embryos injected with a range of *Xnr2* RNA doses [60-600 pg; embryos from Kofron et al. (Kofron et al., 1999)]. We found that high doses of *Xnr2* could strongly inhibit *Xlim5* expression in

Table 1. PCR primer pairs and reaction conditions for real-time RT-PCR

PCR primer pair	Reference	Sequence	Denaturing temperature (°C/seconds)	Annealling temperature (°C/seconds)	Extension temperature (°C/seconds)	Acquisition temperature (°C/seconds)
E-cadherin	New	U, 5′-CGA AGA TGT AAA CGA AGC C-3′; D, 5′-GCC ATT TCC AGT GAC AAT C-3′	95/2	56/5	72/8	83/3
Endodermin	Sasai et al., 1996	U, 5′-TAT TCT GAC TCC TGA AGG TG-3′; D, 5′-GAG AAC TGC CCA TGT GCC TC-3′	95/2	55/5	72/6	81/3
Epidermal keratin	XMMR	U, 5′-CAC CAG AAC ACA GAG TAC-3′; D, 5′-CAA CCT TCC CAT CAA CCA-3′	95/2	55/5	72/9	81/3
Muscle actin	Rupp and Weintraub, 1991	U, 5′-TCC CTG TAC GCT TCT GGT CGT A-3′; D, 5′-TCT CAA AGT CCA AAG CCA CAT A-3′	95/2	55/5	72/12	83/3
NCAM	XMMR	U, 5′-CAC AGT TCC ACC AAA TGC-3′; D, 5′-GGA ATC AAG CGG TAC AGA-3′	95/2	60/5	72/13	84/3
ODC	Heasman et al., 2000	U, 5′-GCC ATT GTG AAG ACT CTC TCC ATT C-3′; D, 5′-TTC GGG TGA TTC CTT GCC AC-3′	95/2	55/5	72/12	83/3
XSlug	New	U, 5′-CCA ATC ACT GTG TGG ACA GG; D, 5′-TGC ATA AGC TGC ACT GGA AC	95/2	58/5	72/8	84/3
Xlim5-UTR	New	U, 5′-CCA ACA GAC AGG CCC AAC-3′; D, 5′-GTG GCT CCG GTG CTA CAG-3′	95/2	60/5	72/8	84/3
Xsox17α	Xanthos et. al., 2001	U, 5′-GCA AGA TGC TTG GCA AGT CG-3′; D, 5′-GCT GAA GTT CTC TAG ACA CA-3′	95/2	58/5	72/8	85/3

XMMR, *Xenopus* Molecular Marker Resource (http://www.xenbase.org/xmmr/Marker_pages/primers.html).

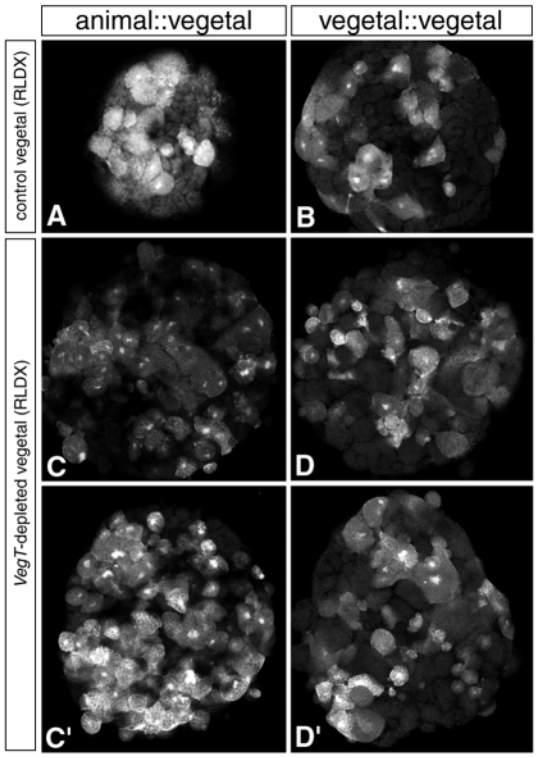

Fig. 1. *VegT*-depleted vegetal cells fail to sort from control animal cap and control vegetal cells. Control vegetal cells injected with RLDX were dissected from stage 9 embryos, dissociated and mixed with unlabelled dissociated animal cap cells (A) or dissociated vegetal cells (B). Aggregates were fixed after 4 hours in culture and viewed by confocal microscopy. Control vegetal cells sort out from animal cells (A) but not from other vegetal cells (B). (C,C′,D,D′) Dissociated, RLDX-labelled *VegT*-depleted vegetal cells from stage 9 embryos were mixed with unlabelled control animal cells (C,C′) or unlabelled control vegetal cells (D,D′). *VegT*-depleted vegetal cells fail to sort out in either case and remain randomly distributed.

VegT-depleted embryos (Fig. 2B), suggesting that the *nodal*-related genes downstream of *VegT* in vegetal cells can repress early ectoderm genes.

Overexpression of Xlim5 in vegetal cells inhibits sorting from animal cells but does not alter germ-layer-specific gene expression

We next asked whether ectopic expression of *Xlim5* was sufficient to change vegetal cell adhesion properties to those of animal cells, and whether it would also induce known ectoderm differentiation markers in vegetal cells, thus mimicking *VegT* depletion. We assayed differential adhesion in blastomere-sorting assays. Embryos were injected vegetally with *Xlim5* RNA (1-2 ng) at the two-cell stage. At the blastula stage (stage 9), vegetal cells were dissociated, mixed with RLDX-labelled animal cells and reaggregated for 4 hours to overnight before fixation. When RLDX-labelled animal cells were mixed with unlabelled vegetal cells, they rapidly sorted from each other and formed distinct populations within the aggregate (Fig. 3A-A″, Fig. 3C). By contrast, when RLDX-labelled animal cells were mixed with *Xlim5*-expressing vegetal cells, the animal cells failed to segregate from the

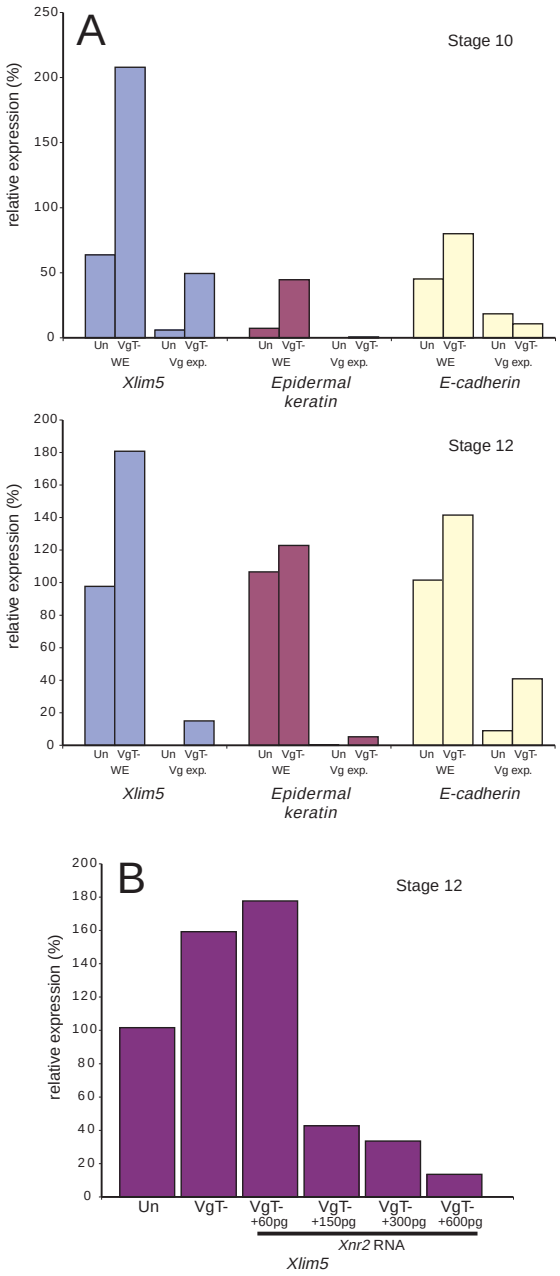

Fig. 2. Expression of the LIM-homeobox gene *Xlim5* is induced in *VegT*-depleted embryos and repressed by *Xnr2*. (A) Vegetal mass explants (Vg exp.) were dissected from stage 9 embryos and cultured to either stage 10 (top) or stage 12 (bottom) along with sibling whole embryos (WE) prior to processing for real-time RT-PCR. Relative expression levels for each gene were determined by comparison to a standard curve generated by serial dilution (100%-10%) of uninjected stage 12 controls. Expression levels of all genes were normalized to the level of *ornithine decarboxylase* (*ODC*) prior to quantitation (not shown). *Xlim5* expression is increased in both *VegT*-depleted whole embryos and vegetal explants. Known ectoderm markers *Epidermal keratin* and *E-cadherin* are included as controls and are also upregulated. (B) *Xlim5* expression is inhibited by *Xnr2* overexpression. *VegT*-depleted embryos and *VegT*-depleted embryos rescued with 60-600 pg of *Xnr2* RNA were analysed by real-time RT-PCR for *Xlim5* expression at stage 12. This cDNA was previously generated for Kofron et al. (Kofron et al., 1999).

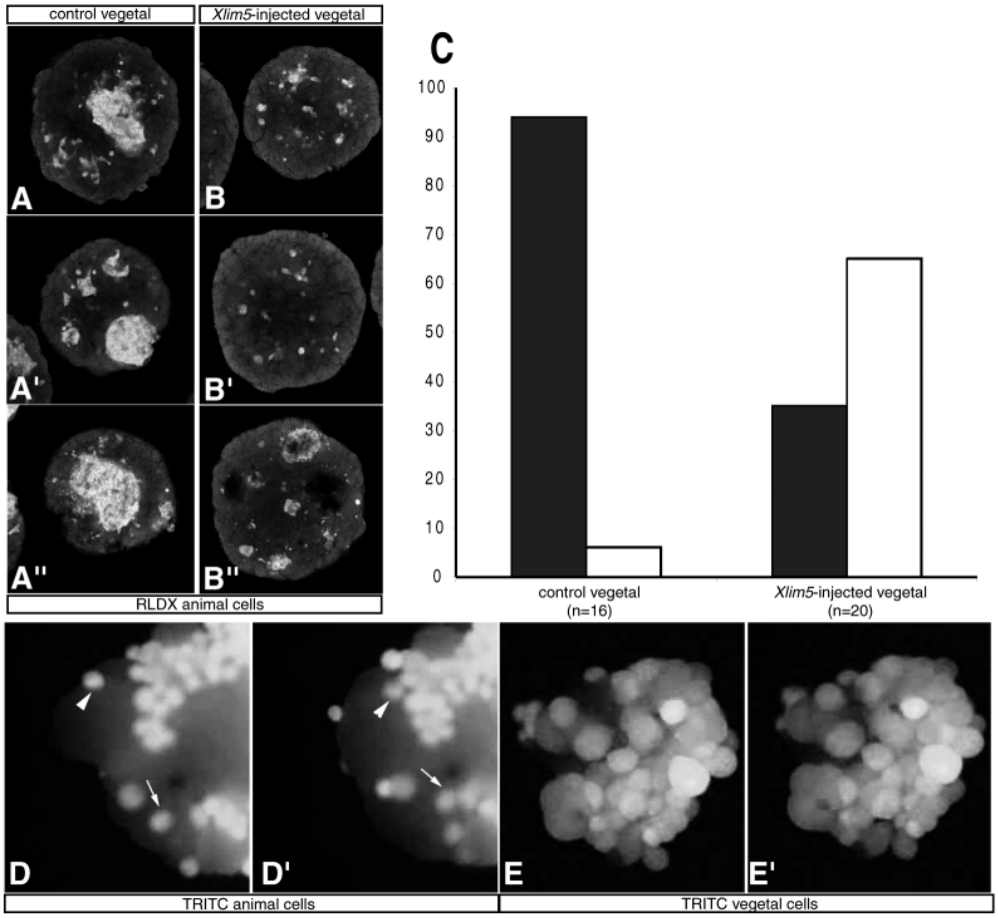

Fig. 3. Xlim5 impairs the sorting of vegetal cells from animal cells. Dissociated animal cap cells injected with RLDX were mixed with uninjected (A-A″) or *Xlim5*-injected (1 ng) (B-B″) vegetal cells and allowed to reaggregate. Aggregates were cleared and viewed by confocal microscopy and scored for sorting. A summary of two experiments is shown in C. Dark grey, positive sorting; white, no sorting. (D,E) Timelapse movies of control animal and vegetal cells in sorting assays. (D,D′) Animal cells labelled with TRITC were aggregated with unlabelled vegetal cells and filmed by timelapse video microscopy. Two animal cells (arrows and arrowheads) are shown moving through the aggregate from a time point ~30 minutes into filming (D) to a time point 3 minutes later (D′). TRITC-labelled vegetal cells aggregated with unlabelled animal cells and filmed over a similar time course do not show any translocation through the aggregate (E,E′).

vegetal cells (Fig. 3B-B″, Fig. 3C). Instead, they formed small clusters or remained as individual cells interspersed among *Xlim5*-injected vegetal cells. As was the case for *VegT* depletion, *Xlim5* expressing vegetal cells did not sort out from uninjected vegetal cells (data not shown).

We next confirmed that the inhibition of sorting in aggregates containing *Xlim5*-injected vegetal cells was due to effects on differential adhesion and not due to effects on motility. We made timelapse movies to determine whether animal cells, vegetal cells or both cell types are motile in our sorting assays. Late blastulae were dissociated and either animal or vegetal cells were labelled with TRITC and timelapse movies of sorting in reaggregates were made using fluorescence microscopy. Using this method we found that animal cells actively move within aggregates during sorting (Fig. 3D-D′), whereas vegetal cells do not move but adhere and maximize contact with each other (Fig. 3E-E′). These results were seen in 3/3 movies using labelled animal cells, and 3/3 movies using labelled vegetal cells. Thus, as vegetal cells are not motile under normal circumstances, inhibition of vegetal cell movement by *Xlim5* cannot account for the impaired sorting activity we observe. Alternatively, Xlim5 could inhibit sorting by conferring motility on vegetal cells. In timelapse movies as described above using *Xlim5*-injected vegetal cells aggregated with control animal cells, we found that this alternative is not the case (data not shown). Taken together these results demonstrate that overexpression of *Xlim5* in vegetal cells is sufficient to activate animal cell-like differential adhesion characteristics in prospective vegetal cells independently of changes in cell motility.

Xlim5 could alter adhesion either by converting vegetal cells to an ectodermal fate or by acting in a more limited role to regulate differential adhesion. To distinguish between these possibilities, we cultured vegetal explants from *Xlim5*-expressing blastulae until the neurula stage and assayed for expression of ectoderm and mesoderm-specific genes. Real-time RT-PCR analysis of stage 22 vegetal explants (Fig. 4) showed that, compared with explants from uninjected embryos, *Xlim5* did not upregulate the expression of ectoderm markers *Epidermal keratin*, *E-cadherin* or *NCAM*, nor markers for mesoderm (*Muscle actin*). The endoderm markers *Endodermin* (*Edd*) and *Xsox17α* were not significantly affected. Thus, at RNA concentrations that affect differential adhesion, ectopic expression of *Xlim5* did not induce ectoderm or mesoderm genes in vegetal explants.

Ectopic expression of *Xlim5* causes vegetal cells to localize to other germ layers in whole embryos

The above results show that *Xlim5* affects vegetal cell adhesion in cell sorting assays in culture. We next asked whether *Xlim5* would cause vegetal cells to segregate to other germ layers in whole embryos. We first injected *Xlim5* RNA into early *Xenopus* embryos and examined the effects on subsequent development. In control embryos, the whole of the epidermis at the neurula stage contains pigment derived from the blastula animal cap (Fig. 5A). In embryos injected vegetally with 2-4

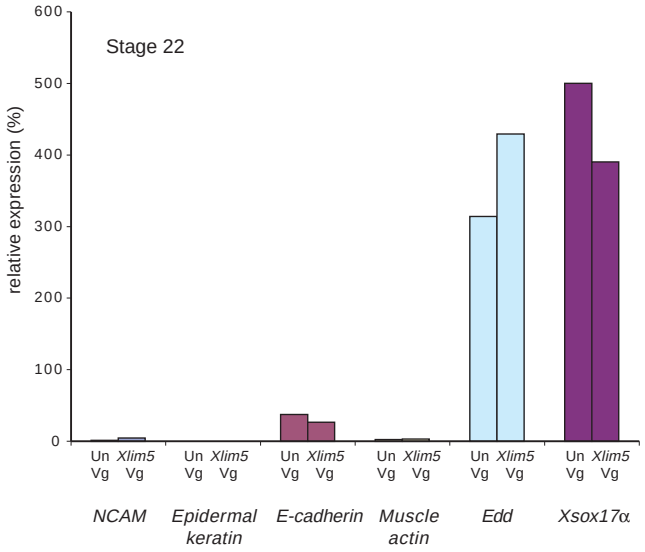

Fig. 4. Xlim5 does not change germ layer-specific gene expression in vegetal endoderm explants. Vegetal masses were dissected from stage 9 embryos either uninjected (Un Vg) or injected with 1 ng of *Xlim5* RNA (*Xlim5* Vg) and cultured until stage 22. Explants were assayed by real-time RT-PCR as described above. Note that ectoderm (*NCAM*, *Epidermal keratin* and *E-cadherin*) and mesoderm (*Muscle actin*) are not induced in *Xlim5*-injected explants. Endoderm markers [*Endodermin* (*Edd*) and *Xsox17α*] are not significantly affected. Relative expression was determined versus stage 22 whole embryos.

ng of *Xlim5* RNA at the two-cell stage, a stunted axis developed and the epidermal layer contained large patches of unpigmented cells that must have arisen from non-animal cells at the blastula stage (Fig. 5B). This phenotype was highly penetrant (50/50 cases) and was never seen in uninjected embryos. In embryos co-injected with *Xlim5* and *β-galactosidase* (*β-gal*) RNA, *lacZ*+ cells were indeed found to populate the mesoderm and epidermis of the embryos, whereas this was not the case in controls injected with *β-gal* alone (data not shown). Embryos injected with RNA doses lower than 2 ng had no obvious phenotype.

To map this change in cell segregation more precisely, we performed lineage analysis by injecting *β-gal* RNA either with or without *Xlim5* RNA (500 pg-1 ng), into one of the ventral vegetal blastomeres of 32-cell embryos (D tier). At the tailbud stage, embryos were fixed, stained for *β-gal* activity and sectioned. In controls injected with *β-gal* alone, staining was mostly limited to cells in the endoderm or lateral plate mesoderm. In embryos co-injected with *β-gal* and *Xlim5*, *β-gal*-labelled cells were found in the neural tube in 5/31 embryos (Table 2, Fig. 5D). These cells were present as individual cells and not part of a large clonal population. In addition, single cells could be seen scattered in the epidermis (13/31 embryos) and dorsal mesoderm tissues (16/31 embryos) (Fig. 5F), although no labelled cells were found in the notochord. In *β-gal*-injected control embryos, labelled cells were not found in the epidermis or in the neural tube and were seen only rarely in the dorsal mesoderm (4/30 embryos) (Fig. 5E). In embryos where labelling was posterior, stained cells were found predominantly in the gut tube in control embryos (Fig. 5G). In *Xlim5*-injected embryos, however, the labelled cells were excluded from the posterior gut and instead

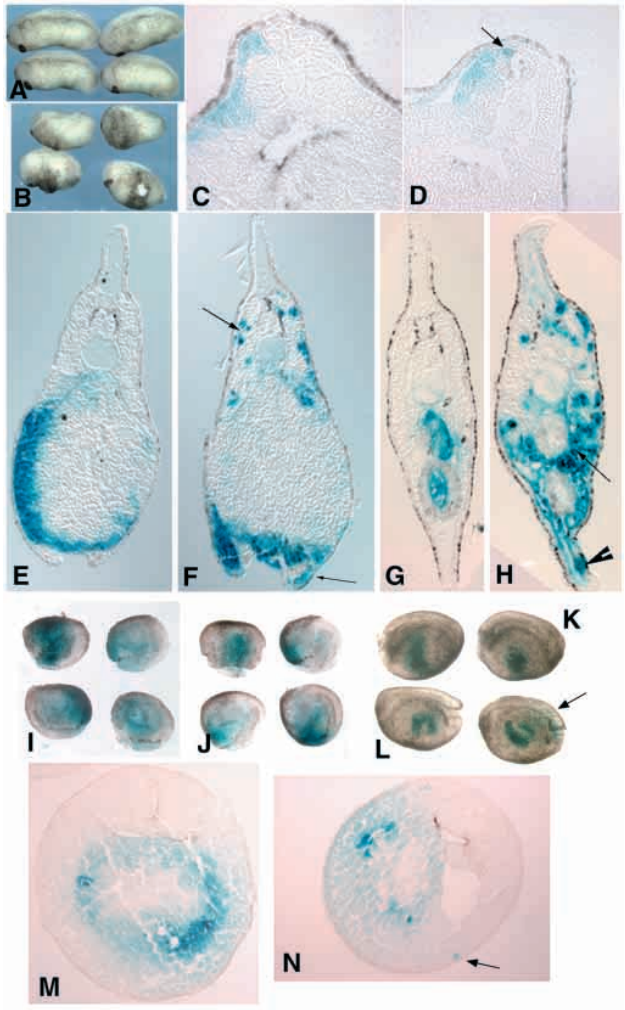

Fig. 5. (A,B) Overexpression of Xlim5 causes vegetal cells to enter other germ layers. (A) Uninjected embryos and (B) embryos injected vegetally with 4 ng *Xlim5* RNA. Note ventral patches of pigmented animal cap cells. (C-H) X-gal staining of tailbud stage embryos injected with *Xlim5* in a vegetal blastomere at the 32-cell stage. Arrows show ectopic locations of *Xlim5*-injected cells in D, F and H. Control embryos injected with *β-gal* alone are shown in C, E and G. Lineage labelling results are summarized in Table 2. (I-N) X-gal staining of late gastrula (I,J) and early neurula stage (L-N) embryos injected with *Xlim5* in a vegetal blastomere at the 32-cell stage. Arrows show ectopic locations of *Xlim5*-injected cells in (L,N). Control embryos injected with *β-gal* alone are shown in I, K and M. Arrowhead in H indicates staining in the ectoderm.

populated the tail mesenchyme and fin epidermis (Fig. 5H). Thus, *Xlim5* caused a region of the vegetal cells to populate other germ layers. This effect was incomplete as many injected cells remained in the endoderm.

We next asked whether the segregation of ectopic cells in *Xlim5*-injected embryos occurred within the time frame of normal germ layer segregation. For these experiments, embryos were fixed at the late gastrula and early neurula stages and stained for *β-gal* activity. We found no evidence of ectopic cells in either control (0/16 embryos; Fig. 5I) or *Xlim5*-injected (0/16 embryos; Fig. 5J) embryos at the mid-gastrula stage (stage 11). Staining was found predominantly in the

Table 2. Xlim5 diverts cells from endoderm to other germ layers

Treatment	Neural	Epidermal	Dorsal mesoderm	Endoderm/ ventral-lateral mesoderm
200 pg β-gal RNA	0/30	0/30	4/30	30/30 (contiguous clones)
200 pg β-gal +500 pg-1 ng Xlim5 RNA	5/31	13/31	16/31	31/31 (scattered cells)

Values indicate number of embryos with indicated staining pattern out of total number examined.

prospective endoderm and lateral plate regions in both sets of embryos. At the neurula stages, however, we were able to observe ectopic cells in *Xlim5*-injected embryos (Fig. 5L). In control *β-gal*-injected embryos staining was mostly in the endoderm (0/15 embryos with ectopic cells; Fig. 5K,M) while in approximately half of the *Xlim5*-injected embryos (9/16 cases; Fig. 5L,N) we saw scattered *lacZ*$^+$ cells located outside a main group of endodermally labelled cells. Thus, the segregation of a population of *Xlim5*-injected vegetal cells occurs during the late gastrula to early neurula stages.

To determine if the ectopic cells injected with *Xlim5* were actually differentiating according to their new location, we performed co-immunostaining experiments. Embryos were injected as above, fixed at the tailbud stage and processed for cryosectioning and immunostaining. Sections were immunostained using mAb 12/101, a marker of mature somites, and an anti-β-galactosidase antibody to identify progeny of the injected cells. In control embryos injected with *β-gal* alone, the somite staining and the β-gal staining were clearly separated (Fig. 6A), while embryos co-injected with *Xlim5* and *β-gal*, a population of cells in the somite were labelled with both antibodies (Fig. 6B, arrow). Thus, overexpression of *Xlim5* in whole embryos is sufficient to cause endodermal cells to relocate to other germ layers and express a tissue-specific marker. This result differs from overexpression of *Xlim5* in isolated endoderm where other germ layer markers were not induced.

Xlim5 loss-of-function

The overexpression experiments above suggested that *Xlim5* controls the differential adhesion properties of animal cells but not other aspects of ectoderm cell fate specification. To determine for which of these processes endogenous *Xlim5* is required in normal development, we used two methods to inhibit its function in whole embryos. We first used an *Xlim5-Engrailed* repressor (*Xlim5-EnR*) fusion construct as a dominant-interfering mutant. We followed a strategy similar to that used by Chan et al. (Chan et al., 2000) and Kodjabachian et al. (Kodjabachian et al., 2001) for Xlim1, in which we replaced the C-terminal domain of Xlim5 with EnR. The C-terminal domain of Xlim1 has been proposed to act as a transcriptional activation domain and we assumed a similar role for the C-terminus of Xlim5. Embryos injected with *Xlim5-EnR* RNA (1 ng) developed normally through the late blastula stage (stage 9) and epiboly of the animal cap was initiated properly at the mid-blastula stage. By stage 10, however, animal cap cells in Xlim5-EnR-injected embryos had completely dissociated while leaving the rest of the embryo intact (Fig. 7B). The timing of animal cell dissociation in Xlim5-EnR-injected embryos correlates well with the onset of *Xlim5* expression in the embryo. *Xlim5* transcripts begin to accumulate at stage 9 and reach a peak of expression at about stage 12 and cell dissociation occurs within this same time frame. Uninjected embryos did not show any cell dissociation (0/50; 0%; Fig. 7A), whereas most *Xlim5-EnR*-injected embryos were dissociating (26/30; 86%; Fig. 7B) by the mid-gastrula stage.

As a test of specificity, we co-injected *Xlim5-EnR* with wild-type *Xlim5* RNA (1 ng) and were able to dramatically reduce the number of dissociating animal caps (4/32; 12.5%; Fig. 7C). *Xlim5-EnR* causes cell dissociation specifically in animal cells, as injection into oocytes followed by host transfer to express Xlim5-EnR uniformly only causes animal and some equatorial cells to dissociate (Fig. 7G). Injection of *Xlim5-EnR* into vegetal cells had no effect, so the cell dissociation cannot be a nonspecific effect of the construct. In addition, the effects of *Xlim5-EnR* are not likely to result from interference with other LIM family members as a similar *Xlim1-EnR* construct was reported to cause anterior truncations and not cell dissociation (Chan et al., 2000; Kodjabachian et al., 2001).

We further showed that Xlim5 was important for proper adhesion in the ectoderm by performing lineage analysis. Injection of *β-galactosidase* (*β-gal*) RNA into animal blastomeres at the 32-cell stage (A tier) labelled a scattered population of epidermal cells (Fig. 7D). However, when *Xlim5-EnR* RNA was co-injected with *β-gal*, epidermal staining was lost and injected cells formed distinct clumps either in the pharyngeal cavity or in the endoderm (Fig. 7E). We next performed reaggregation assays to show that *Xlim5-EnR* specifically disrupts cell adhesion. Animal caps were dissected from control or *Xlim5-EnR*-injected embryos at stage 9 and dissociated in Ca^{2+} and Mg^{2+}-free meduim. Dissaggregated blastomeres were then transferred into OCM and allowed to reaggregate until stage 11. Control cells formed either large

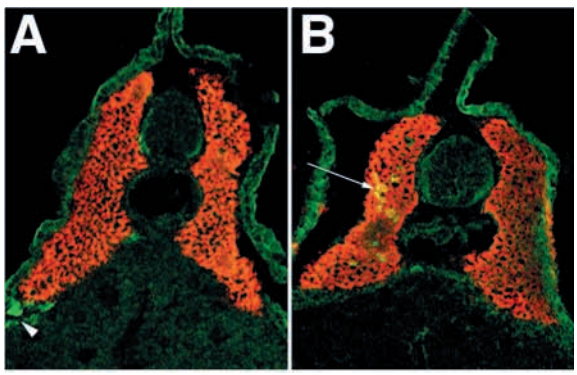

Fig. 6. Ectopic *Xlim5*-expressing cells express a marker of mature somites. Embryos injected with either *β-gal* RNA alone (A) or *β-gal* + *Xlim5* RNA (B) vegetally at the 32-cell stage were fixed at the tailbud stage and immunostained after cryosectioning. Sections were stained with mAb 12/101 (somite, red) along with an antibody against β-galactosidase (green). Embryos injected with *β-gal* alone show non-overlapping staining of 12/101 with β-gal (arrowhead) while a population of *Xlim5*-co-injected cells shows colocalization of the two antibodies (arrow, yellow). The slight green staining in the epidermis is due to background staining.

aggregates or smaller clumps of two to four cells when incubated in Ca^{2+} and Mg^{2+}--containing medium (Fig. 7G). *Xlim5-EnR*-injected cells in contrast remained dissociated or formed only small aggregates (Fig. 7H).

Because *Xlim5-EnR*-injected cells could dissociate due to cell death, we stained dissaggregated cells with Sytox Green to identify dead cells. Few control or *Xlim5-EnR*-injected cells showed any detectable Sytox Green staining (Fig. 7I,J). By contrast, cells killed by incubation in distilled water as a positive control were abundantly stained. These results argue that the cell dissociation seen in *Xlim5-EnR*-injected embryos is not due to abnormal cell migration or cell death. As *Xlim5* is overexpressed in *VegT*-depleted vegetal cells, we next wanted to assess the contribution of *Xlim5* to the overall phenotype of *VegT*-depleted embryos. We injected *Xlim5-EnR* RNA into the vegetal poles of *VegT*-depleted embryos to attempt to restore a normal phenotype. However, the *VegT*-depleted vegetal cells, which are converted to ectoderm, began to dissociate in a similar manner as *Xlim5-EnR*-injected animal cells (data not shown).

The above observations provide evidence that Xlim5 is required for proper cell adhesion within the ectoderm. However, active repression of Xlim5-regulated genes via the Engrailed repressor domain may produce more severe effects than if Xlim5 were simply not present. We therefore attempted to block *Xlim5* function using morpholino antisense oligos (MO). Xlim5-MO-injected (40-50 ng Xlim5 MO) embryos appeared to develop normally through the gastrula stage before showing a profound delay in the formation of the neural plate and subsequent neural folds. The delay is particularly evident at the neural tube closure stage when the majority of MO-injected embryos have failed to close the anterior part of the neural tube. To test the specificity of the Xlim5-MO we co-injected *Xlim5* RNA along with the MO and assayed neural tube closure at stage 18. Xlim5-MO-injected embryos failed to complete neural fold closure (Fig. 7L, middle row, 9/50 normal closure) at the same time as controls (Fig. 7L, top row, 60/60 normal closure); however, the majority of rescued embryos had closed their neural folds (Fig. 7L, bottom row, 28/50 normal closure).

To determine if the delay in neural plate development was due to a loss of neural fate, we assayed molecular markers at the gastrula stage by real time RT-PCR (Fig. 7M). We found that both epidermal and neural markers

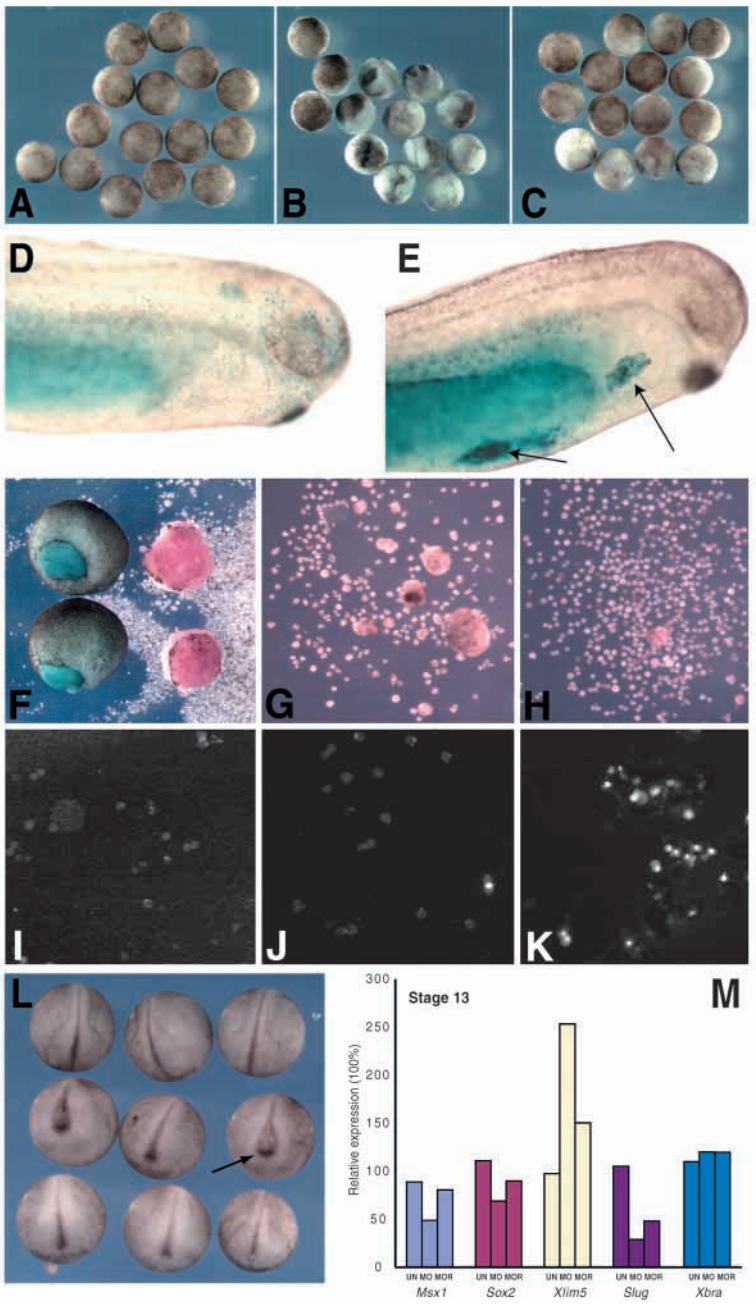

Fig. 7. Inhibition of Xlim5 interferes with normal ectoderm development. (A-C) Injection of *Xlim5-EnR* causes cell dissociation during gastrulation. (A) Uninjected stage 10.5 embryos. (B) Sibling embryos injected with 1 ng *Xlim5-EnR* RNA. Note the number of embryos with non-uniform pigment and white patches indicating dissociated cells. (C) Rescued embryos co-injected with 1 ng *Xlim5-EnR* + 1 ng *Xlim5*. Embryos have recovered normal adhesion. (D,E) Injection of *Xlim5-EnR* into animal blastomeres inhibits ectoderm adhesion. (D) Injection of *β-gal* into a ventral-animal blastomere at the 32-cell stage. Labelled cells populate the epidermis (scattered blue cells). (E) Co-injection of *β-gal* with 100 pg *Xlim5-EnR*. Cells are lost from the epidermis and form clumps in the pharynx and gut (arrows). (F) Uninjected (left, blue) and *Xlim5-EnR*-injected embryos (right, red) obtained by the host transfer technique showing dissociation of animal and equatorial cells but not vegetal cells. (G,H) Control (G) or *Xlim5-EnR*-injected (H) animal cap cells were dissociated and reaggregated in OCM. Large aggregates are formed in the controls but are absent in the *Xlim5-EnR*-injected cells. (I-K) Sytox Green staining of dissociated cells. Uninjected (I) and *Xlim5-EnR*-injected cells (J) do not stain with Sytox Green, whereas positive control dead cells (K) stain brightly. (L) Depletion of Xlim5 with an antisense MO delays neural fold morphogenesis. (Top) Uninjected control embryos at stage 18. (Middle) Sibling embryos injected with 40 ng Xlim5-MO. Notice open anterior neural folds (arrow). (Bottom) MO-injected embryos injected with 1 ng *Xlim5* RNA. Neural fold closure is rescued in these embryos. (M) Ectoderm marker gene expression in Xlim5-MO injected embryos assayed by real-time RT-PCR. UN, uninjected stage 13 embryos; MO, 40 ng Xlim5-MO; MOR, 40 ng Xlim5-MO + 1 ng *Xlim5* RNA.

Msx1 and *Sox2* were slightly reduced in expression, while *Xslug*, a neural crest marker, was severely reduced in expression. *Xbra*, a marker for posterior mesoderm and notochord at this stage, was unaffected. Surprisingly *Xlim5* itself was increased, suggesting that Xlim5 might regulate its own expression by a negative-feedback mechanism. At later stages (stage 18), ectoderm markers (*Epidermal keratin*, *NCAM*, *E-cadherin*) were still slightly affected but returned to near normal levels (data not shown). Exogenous *Xlim5* RNA rescued the effects of the Xlim5-MO on gene expression, confirming the specificity of these effects. This RNA does not contain the MO-binding site, thus rescue is by replacement of Xlim5 and not by MO competition. Overall, the loss of animal cell adhesion in *Xlim5-EnR*-injected embryos and the abnormal neural fold morphogenesis in Xlim5-MO-injected embryos further suggest that Xlim5 is important in the proper development, although not the initial specification, of the ectoderm.

DISCUSSION

In this work we describe the role of Xlim5, a LIM-homeodomain protein, in mediating cell adhesion and morphogenesis in the ectoderm. We focused on Xlim5 because it is upregulated in *VegT*-depleted vegetal explants, which lack mesoderm and endoderm gene expression and ectopically express ectoderm genes. We show that Xlim5 overexpression in endodermal cells can alter their adhesion properties and ultimate location in the embryo. This is accomplished without wholesale activation of ectoderm markers. Furthermore, we find that interfering with the function of Xlim5 in embryos leads to defects in ectoderm-specific cell sorting but does not block initial formation of the ectoderm germ layer. These results argue that Xlim5 regulates a set of genes involved in establishing the adhesive and migratory properties of ectoderm cells independently of regulation of their initial cell fate.

Role of *Xlim5* in germ layer development

The T-box transcription factor VegT is required in *Xenopus* for the specification of endoderm in vegetal cells and for the expression of molecules that induce mesoderm in equatorial cells. In previous work, we have found that ectoderm-specific genes were ectopically expressed in equatorial and vegetal cells of *VegT*-depleted embryos (Zhang et al., 1998). Here, we extend those observations by showing that ectoderm genes are activated during gastrula stages in the vegetal cells of *VegT*-depleted embryos. In addition, we find that uninjected animal cap cells do not sort from *VegT*-depleted vegetal cells. These results argue that loss of *VegT* (and subsequent Nodal signalling) is sufficient to activate ectoderm differentiation in vegetal cells. However, in vegetal:vegetal sorting assays *VegT*-depleted cells or vegetal cells expressing *Xlim5* remained randomly mixed with control vegetal cells. Surprisingly, in timelapse movies of cell sorting, we found that vegetal cells are inherently non-motile during the early gastrula stage, while animal cells are highly motile. This lack of motility could be due to the presence of a vegetally localized molecule that blocks cell movement. Alternatively, the large size of vegetal cells at this stage could prevent efficient cell motility despite the expression of ectoderm adhesion molecules.

In current models for germ layer determination, high levels of VegT/TGF-β signalling specifies endoderm, medium levels induce mesoderm and the absence of TGF-β signalling results in ectoderm. Our results are consistent with this model in general, as we find that the LIM-homeodomain gene *Xlim5*, an early marker for ectoderm (Toyama et al., 1995), is activated in the absence of *VegT* and is repressed by *Xnr2*. However, overexpression of *Xlim5* in vegetal cells does not recapitulate *VegT* depletion with regard to activation of differentiated ectoderm markers. Other transcription factors upregulated in *VegT*-depleted embryos, as yet unknown, must be responsible for inducing ectoderm-specific gene expression in vegetal cells. Unfortunately, we were unable to determine whether blockage of ectopic *Xlim5* in *VegT*-depleted vegetal cells could restore normal development because of the subsequent dissociation of these cells. In this work, both gain- and loss-of-function approaches support an alternate role for *Xlim5* specifically in regulating cell adhesion.

Role of Xlim5 in regulating differential adhesion

The role of LIM-HD proteins in regulating cell adhesion independently of cell fate has several parallels in development (Hukriede et al., 2003; Kania et al., 2000; Zhao et al., 1999). Gene targeting of the Xlim5 homologue, *Lhx5*, in mice causes a failure in the migration and differentiation of hippocampal cell precursors (Zhao et al., 1999). Although the nature of the defect in this case is not clear, the abnormal migration indicates that adhesion may be affected in these cells. Recently, in *Xenopus*, the closely related *Xlim1* gene was shown to be required for cell movements during gastrulation mediated by regulation of *paraxial protocadherin* (*PAPC*) (Hukriede et al., 2003). Interestingly, expression of organizer genes and neuroectoderm markers were essentially normal in *Xlim1*-depleted embryos, suggesting that the major defect is in cell movement or adhesion. In addition, disruption of *Lim1*, a gene highly similar to *Lhx5*, in a subset of motoneurones caused inappropriate axon targeting to dorsoventral compartments of the limb muscle (Kania et al., 2000). In this case, the mis-targeting of $Lim1^{-/-}$ axons occurred without overall loss of motoneurone identity. In dissociated cells and explants, we show that *Xlim5* can alter adhesion without inducing ectoderm markers. By contrast, lineage-labelling experiments in intact embryos show that ectopic *Xlim5*-injected vegetal cells go on to express markers of the surrounding tissue. One explanation for this apparent discrepancy could be that *Xlim5* causes inappropriate adhesion of vegetal cells to other germ layers early in development. Subsequently, injected cells might come under the influence of germ layer-specific or tissue-specific inducing molecules and then differentiate according the surrounding cells. Our lineage-labelling experiments in late gastrula and early neurula embryos support this idea. We do not find evidence for any ectopic cells at the gastrula stage, after regional specification of germ layers has taken place. However, we do find ectopic *Xlim5*-injected cells by the neurula stage after significant morphogenetic events have taken place. The most likely explanation for these observations is that *Xlim5*-injected cells adhere to an inappropriate germ layer and then are carried with that tissue during morphogenesis.

In *Xlim5* loss-of-function experiments, we also find evidence for altered cell adhesion in the ectoderm without overall loss of ectoderm fate. Injection of the *Xlim5-EnR* construct causes animal cells to dissociate. By contrast, inhibition of *Xlim5*

translation with a MO causes a delay in neural fold morphogenesis. Without a specific antibody to determine the extent of protein depletion in MO-injected embryos it is difficult to say whether these two effects are qualitatively different. In addition, because the Xlim5-MO increases *Xlim5* expression, the efficiency of the MO is likely to decrease during development and allow normal morphogenesis to occur. Alternatively, an *Xlim5* pseudoallele (*X. laevis* is allotetraploid) may exist that is not targeted by the MO. Although we have not found another *Xlim5* allele either by PCR or through database searches, we cannot rule out its existence. It may be preferable to carry out these experiments in the diploid *Xenopus tropicalis* to avoid problems with pseudoalleles. The effects of MO injection were rescued by injection of *Xlim5* RNA, showing that the defects, however subtle, are in fact specific to inhibition of *Xlim5*. Overall, we have shown through two different methods that interfering with *Xlim5* function impairs normal ectoderm adhesion without a loss of ectoderm marker expression.

Some key questions arising from this work are: what adhesion molecules are regulated by Xlim5 and what role could the uncoupling of initial cell fate specification from adhesion play in normal development? To address the second question, activation of a germ layer-specific adhesion program independent of specification could serve to sharpen germ layer boundaries by allowing animal cells that receive low doses of inducing factors to still migrate to the correct tissue. Adhesion factors potentially regulated by *Xlim5* include members of the cadherin and protocadherin families as well as Eph receptors and ephrin ligands, which have been implicated in mediating cell adhesion and migration (Holder and Klein, 1999). Interestingly, inhibition of NF-protocadherin, an ectoderm-specific protocadherin (Bradley et al., 1998), or activation of Ephrin B1 signalling (Jones et al., 1998) both produce cell dissociation effects similar to *Xlim5-EnR* injection. This possibility is intriguing given the recent demonstration that *Xlim1* regulated expression of *PAPC* (Hukriede et al., 2003). Finally, it will be important to identify maternal factors involved in regulating *Xlim5* expression in order to establish a genetic hierarchy of ectoderm development.

The authors thank the Kenneth Campbell laboratory for help with cryosections, and Janet Heasman and Henrietta Standley for critical reading of the manuscript. The monoclonal antibody 12/101 developed by J. P. Brockes was obtained from the Developmental Studies Hybridoma Bank developed under the auspices of the NICHD and maintained by The University of Iowa, Department of Biological Sciences, Iowa City, IA 52242. This work was supported by NIH NRSA F32 HD40716-01 (to D.W.H.) and the William Schubert Endowment (to C.W.).

REFERENCES

Bradley, R. S., Espeseth, A. and Kintner, C. (1998). NF-protocadherin, a novel member of the cadherin superfamily, is required for Xenopus ectodermal differentiation. *Curr. Biol.* **8**, 325-334.

Chan, T. C., Takahashi, S. and Asashima, M. (2000). A role for Xlim-1 in pronephros development in Xenopus laevis. *Dev. Biol.* **228**, 256-269.

Heasman, J. (1997). Patterning the Xenopus blastula. *Development* **124**, 4179-4191.

Heasman, J., Wylie, C. C., Hausen, P. and Smith, J. C. (1984). Fates and states of determination of single vegetal pole blastomeres of X. laevis. *Cell* **37**, 185-194.

Heasman, J., Kofron, M. and Wylie, C. (2000). Beta-catenin signalling activity dissected in the early Xenopus embryo: a novel antisense approach. *Dev. Biol.* **222**, 124-134.

Henry, G. L., Brivanlou, I. H., Kessler, D. S., Hemmati-Brivanlou, A. and Melton, D. A. (1996). TGF-beta signals and a pattern in Xenopus laevis endodermal development. *Development* **122**, 1007-1015.

Hobert, O. and Westphal, H. (2000). Functions of LIM-homeobox genes. *Trends Genet.* **16**, 75-83.

Holder, N. and Klein, R. (1999). Eph receptors and ephrins: effectors of morphogenesis. *Development* **126**, 2033-2044.

Hukriede, N. A., Tsang, T. E., Habas, R., Khoo, P.-L., Steiner, K., Weeks, D. L., Tam, P. P. L. and Dawid, I. (2003). Conserved requirement of Lim1 function for cell movements during gastrulation. *Dev. Cell* **4**, 83-94.

Jones, T. L., Chong, L. D., Kim, J., Xu, R. H., Kung, H. F. and Daar, I. O. (1998). Loss of cell adhesion in Xenopus laevis embryos mediated by the cytoplasmic domain of XLerk, an erythropoietin-producing hepatocellular ligand. *Proc. Natl. Acad. Sci. USA* **95**, 576-581.

Kania, A., Johnson, R. L. and Jessell, T. M. (2000). Coordinate roles for LIM homeobox genes in directing the dorsoventral trajectory of motor axons in the vertebrate limb. *Cell* **102**, 161-173.

Kodjabachian, L., Karavanov, A. A., Hikasa, H., Hukriede, N. A., Aoki, T., Taira, M. and Dawid, I. B. (2001). A study of Xlim1 function in the Spemann-Mangold organizer. *Int. J. Dev. Biol.* **45**, 209-218.

Kofron, M., Demel, T., Xanthos, J., Lohr, J., Sun, B., Sive, H., Osada, S., Wright, C., Wylie, C. and Heasman, J. (1999). Mesoderm induction in Xenopus is a zygotic event regulated by maternal VegT via TGFbeta growth factors. *Development* **126**, 5759-5770.

Kofron, M., Klein, P., Zhang, F., Houston, D. W., Schaible, K., Wylie, C. and Heasman, J. (2001). The role of maternal axin in patterning the Xenopus embryo. *Dev. Biol.* **237**, 183-201.

Lemaire, P. and Gurdon, J. B. (1994). A role for cytoplasmic determinants in mesoderm patterning: cell- autonomous activation of the goosecoid and Xwnt-8 genes along the dorsoventral axis of early Xenopus embryos. *Development* **120**, 1191-1199.

Muñoz-Sanjuan, I. and Brivanlou, A. H. (2002). Neural induction, the default model and embryonic stem cells. *Nat. Rev. Neurosci.* **3**, 271-280.

Rupp, R. A. and Weintraub, H. (1991). Ubiquitous MyoD transcription at the midblastula transition precedes induction-dependent MyoD expression in presumptive mesoderm of X. laevis. *Cell* **65**, 927-937.

Ryan, K., Garrett, N., Mitchell, A. and Gurdon, J. B. (1996). Eomesodermin, a key early gene in Xenopus mesoderm differentiation. *Cell* **87**, 989-1000.

Sasai, Y., Lu, B., Piccolo, S. and de Robertis, E. M. (1996). Endoderm induction by the organizer-secreted factors chordin and noggin in Xenopus animal caps. *EMBO J.* **15**, 4547-4555.

Snape, A., Wylie, C. C., Smith, J. C. and Heasman, J. (1987). Changes in states of commitment of single animal pole blastomeres of Xenopus laevis. *Dev. Biol.* **119**, 503-510.

Toyama, R., Curtiss, P. E., Otani, H., Kimura, M., Dawid, I. B. and Taira, M. (1995). The LIM class homeobox gene lim5: implied role in CNS patterning in Xenopus and zebrafish. *Dev. Biol.* **170**, 583-593.

Turner, A., Snape, A. M., Wylie, C. C. and Heasman, J. (1989). Regional identity is established before gastrulation in the Xenopus embryo. *J. Exp. Zool.* **251**, 245-252.

Wilson, P. A. and Hemmati-Brivanlou, A. (1995). Induction of epidermis and inhibition of neural fate by Bmp-4. *Nature* **376**, 331-333.

Wylie, C. C., Snape, A., Heasman, J. and Smith, J. C. (1987). Vegetal pole cells and commitment to form endoderm in Xenopus laevis. *Dev. Biol.* **119**, 496-502.

Xanthos, J. B., Kofron, M., Wylie, C. and Heasman, J. (2001). Maternal VegT is the initiator of a molecular network specifying endoderm in Xenopus laevis. *Development* **128**, 167-180.

Yasuo, H. and Lemaire, P. (1999). A two-step model for the fate determination of presumptive endodermal blastomeres in Xenopus embryos. *Curr. Biol.* **9**, 869-879.

Zhang, J., Houston, D. W., King, M. L., Payne, C., Wylie, C. and Heasman, J. (1998). The role of maternal VegT in establishing the primary germ layers in Xenopus embryos. *Cell* **94**, 515-524.

Zhao, Y., Sheng, H. Z., Amini, R., Grinberg, A., Lee, E., Huang, S., Taira, M. and Westphal, H. (1999). Control of hippocampal morphogenesis and neuronal differentiation by the LIM homeobox gene Lhx5. *Science* **284**, 1155-1158.

Zuck, M. V., Wylie, C. C. and Heasman, J. (1998). Maternal mRNAs in *Xenopus* embryos: an antisense approach. In *A Comparative Methods Approach to the Study of Oocytes and Embryos* (ed. J. D. Richter), pp. 341-354. Oxford: Oxford University Press.